Article ECORFAN Journal Democratic Republic of Congo
December 2020 Vol.6 No.11 1-11

Methodology to calculate the density of the magnetic field generated in overhead transmission lines in HVDC applying a two-dimensional analysis of parallel poles above ground level

Metodología para calcular la densidad del campo magnético generado en líneas de transmisión aéreas en HVDC aplicando un análisis bidimensional de polos paralelos sobre el nivel del suelo

AGUILAR-MARIN, Jorge Luis†*, CISNEROS-VILLALOBOS, Luis, PADILLA-CANTERO, Jorge Gabriel and VERGARA-VÁZQUEZ, Julio Cesar

Universidad Autónoma del Estado de Morelos, Faculty the Chemical Sciences and Engineering, Av. University 1001, Cuernavaca, Morelos, C.P. 62209, Mexico.

ID 1st Author: *Jorge Luis, Aguilar-Marin* / **ORC ID:** 0000-0002-0235-6946, **Researcher ID:** ABD-4533-2020, **CVU CONACYT ID:** 1010823

ID 1st Co-author: *Luis, Cisneros-Villalobos* / **ORC ID:** 0000-0002-9409-1374, **Researcher ID:** ABD-4724-2020, **CVU CONACYT ID:** 82259

ID 2nd Co-author: *Jorge Gabriel, Padilla-Cantero* / **ORC ID:** 0000-0002-6414-9483, **Researcher ID:** ABD-5334-2020

ID 3rd Co-author: *Julio Cesar, Vergara-Vázquez* / **ORC ID:** 0000-0003-1524-7914, **Researcher ID:** ABD-5487-2020

DOI: 10.35429/EJDRC.2020.6.11.1.11 Received July 10, 2020; Accepted December 30, 2020

Abstract

The growth in the demand for electricity has led to the development and application of technologies that make its means of transport more efficient. Thus, one of these options is the implementation of transmission lines in HVDC. One of important design parameters of these lines is to know their magnetic field distribution, when it is required to calculate it, there is no methodology that can be applied to HVDC transmission lines. The following article presents a methodology that allows obtaining the density of the magnetic field on the corridor of an overhead transmission line. A case study of a 500 kV bipolar line in HVDC is presented, the results obtained are compared using the commercial software Field and corona Effects (FACE), the results obtained are consistent with those obtained from the presented methodology. An analysis of the impact of the transmission line configuration on the magnetic field density is developed, defining the most efficient configuration.

HVDC, Imaginary poles, Line runner

Resumen

El crecimiento de la demanda de energía eléctrica ha provocado el desarrollo y la aplicación de tecnologías que hacen más eficiente su medio de transporte. Así una de estas operaciones es la implementación de líneas de transmisión en HVDC. Uno de los parámetros importantes de diseño de estas líneas es conocer su distribución de su campo magnético, cuando se requiere calcularlo no se cuenta con una metodología que pueda ser aplicada en las líneas de transmisión en HVDC. El siguiente artículo presenta una metodología que permite la obtención de la densidad del campo magnético sobre el corredor de una línea de transmisión aérea. Se presenta un caso de estudio de una línea bipolar de 500 kV en HVDC, los resultados obtenidos son comparados por medio del software comercial Field and Corona Effects (FACE), los resultados obtenidos son coherentes con los obtenidos a partir de la metodología presentada. Se desarrolla un análisis del impacto de la configuración de la línea de transmisión en la densidad de campo magnético, definiendo la configuración más eficiente.

HVDC, Polos imaginarios, Corredor de línea

Citation: AGUILAR-MARIN, Jorge Luis, CISNEROS-VILLALOBOS, Luis, PADILLA-CANTERO, Jorge Gabriel and VERGARA-VÁZQUEZ, Julio Cesar. Methodology to calculate the density of the magnetic field generated in overhead transmission lines in HVDC applying a two-dimensional analysis of parallel poles above ground level. Journal - Democratic Republic of Congo. 2020. 6-11:1-11.

* Correspondence to Author (Email: jorge.aguilar.itt@gmail.com)
† Researcher contributing as first author.

Introduction

Today, one of the most efficient methods for the transmission of electrical energy is to use High Voltage Direct Current (HVDC), when it comes to providing electrical energy from long distances to a large load and that is in continuous growth (Lee, Pong & Zhu, 2019), (Tang, Luo & Wei, 2013), (Feltes, Gemmell & Retzmann, 2011).

Due to the remarkable increase in the power and reliability of AC/DC power converters, the transmission of high voltage power in HVDC has grown significantly worldwide. Currently, the voltages used for overhead transmission are in the range of ±500 to ±800 kV, with nominal currents of 1 to 4 kA (Girdinio, Molfino, Nervi, Rossi, Bertani & Malgarotti, 2015), (Baharman & Johnson, 2007).

The below the main ones are listed technical benefits of an HVDC system (Samy, 2017).

– The energy flow is fully controllable, fast and accurate.

– The link in HVDC is asynchronous and can adapt to any nominal voltage or frequency.

– Transmission lines in HVDC do not increase the short-circuit level of the system and faults cannot be transferred through connections in HVDC.

– There is a better ability to transmit power with overhead, underground and submarine cables over long distances.

– The visual impact and the use of the land is lower, as well as the cost for the line corridor (Mooney, 2010).

In Figure 1 the dimensions of the land used for transmission line are observed HVAC and an HVDC (Zhou, Qiu, Sun, Chen, Deng, Qian, Wang, Zhao, Li, Li, Qiu & Yu, 2018).

Currently Mexico does not have transmission systems in HVDC and with the growing demand for energy, it will be one of the most efficient transmission media in the near future, so this technology is being analysed by Mexican regulations, for the development of the National Electric System (SEN), with regard to generation and transmission activities (PROSEDEN, 2019).

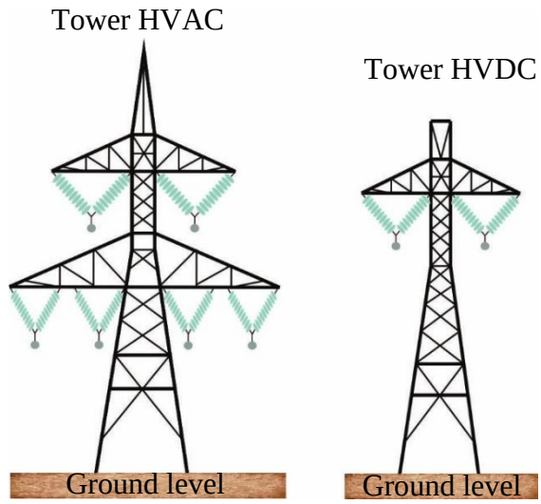

Figure 1 High voltage structures in HVAC and HVDC
Source: Own elaboration

One of the important parameters for the design of HVDC lines is the magnetic field is caused by the circulation of electric current in a conductor (Jang, Kim, Lee, Lim & Sood, 2009), (Rofalski & Schlabbach, 2014). Figure 2 shows its distribution around a conductor, so the magnetic field generated in transmission lines is determined by the magnitude of the current that circulates through the conductors and by the spatial configuration of the line (IEC, 2014).

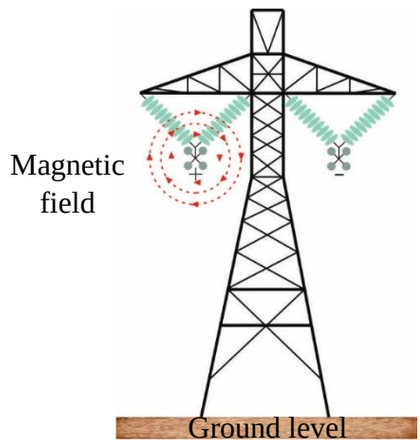

Figure 2 Magnetic field in a bipolar transmission line in HVDC
Source: Own elaboration

ISSN: 2414-4924

AGUILAR-MARIN, Jorge Luis, CISNEROS-VILLALOBOS, Luis, PADILLA-CANTERO, Jorge Gabriel and VERGARA-VÁZQUEZ, Julio Cesar. Methodology to calculate the density of the magnetic field generated in overhead transmission lines in HVDC applying a two-dimensional analysis of parallel poles above ground level. Journal - Democratic Republic of Congo. 2020

In the case of HVDC systems the frequency is null, therefore is it considered 0 Hz, according to the Carson method (Zhu, Lee & Pong, 2018). The image conductor will be located at a great depth below ground level as seen in Figure 3 and the equivalent distance of the image conductor will tend to infinity (IEC, 2014) therefore, the effect of the image conductors is so small that can despised for the calculation of the magnetic field density in HVDC transmission lines.

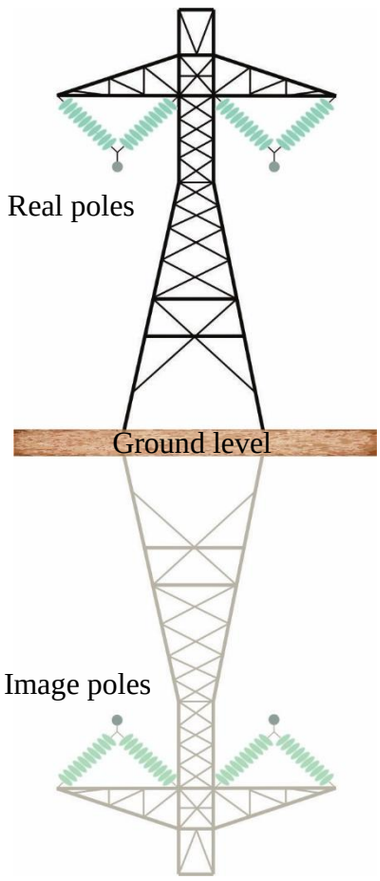

Figure 3 Carson´s method, imaginary poles.
Source: Own elaboration

At present there are multiple software is that present the calculation of the magnetic field density of HVDC transmission lines such as CRmag, FACE, ETAP, among others. However, most require the purchase of licenses for their operation.

This software's are based, on the method complex penetration, which uses Carson´s method that consists of the circulation of a current that returns overland, this method considers the ground as a superconductor, based on the phenomenon of the skin effect or complex penetration effect, with which the return of the current through the ground is modelled.

The complex penetration effect considers that the magnetic field lines cross the surface of the soil, where for the calculation magnetic field density the equivalent complex reference plane is considered, which is at a great depth, to know this depth. The parameter α related to the skin depth or complex penetration depth, or the distance from the ground level surface to the reference plane is incorporated (Sarma, 2000).

The following article provides engineers with a reference methodology, which contains the steps necessary to calculate the magnetic field density for the first overhead transmission lines in HVDC to be built in Mexico. The density of the magnetic field is obtained by applying a two-dimensional analysis of the transmission line, assuming parallel poles above ground level, considering the operating characteristics of the line and, unlike other methodologies, the exposure limits to magnetic fields are taken into account recommended by (ICNIRP, 2009). The methodology offers speed and precision in calculating the density of the magnetic field over the corridor of a monopolar and bipolar transmission line.

Calculation methodology for density of magnetic field

The following methodology allows calculate the components of the magnetic field density in a simplified but reasonably exact way over the corridor of an overhead transmission line in HVDC, the design is based mainly on complying with the limits for exposure to magnetic fields. The flow chart of the methodology is presents itself ted in Figure 4.

ISSN: 2414-4924

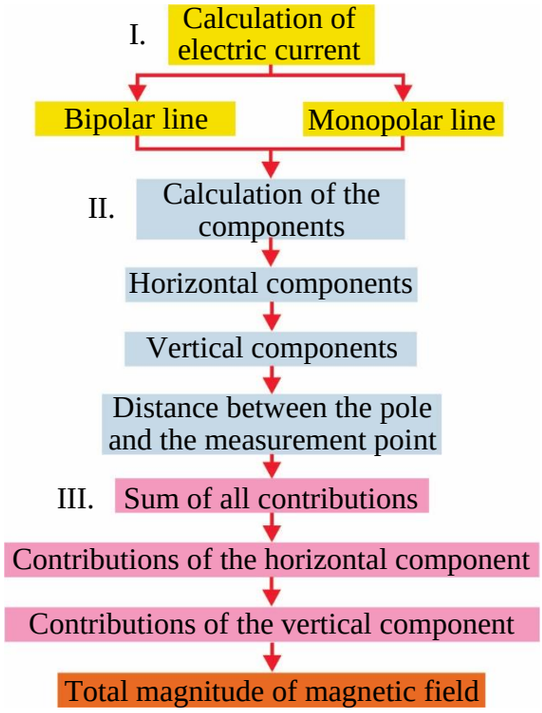

Figure 4 Process for calculating the magnetic field density in HVDC transmission lines
Source: Own elaboration

Calculation of the electric current

The calculation of electric current intensity for transmission lines in monopolar and bipolar HVDC It is determined through the equations (1) and (2), respectively (CIGRE, 2014).

$$I = \frac{1}{2} \cdot \left(\frac{P \times 10^3}{V}\right) A \quad (1)$$

$$I = \left(\frac{P \times 10^3}{V}\right) A \quad (2)$$

Where:

I = Electric Current of the pole, in A.
P = Power of the line, in MW.
V = Electrical voltage of the pole, in kV.

The current intensity will considered positive, when evaluating the positive pole and negative when considering the negative pole (CIGRE, 2014).

Calculation of horizontal and vertical components

To determine the components of the magnetic field density, the following considerations must taken.

- The currents at the poles of transmission lines in HVDC are of different polarity, which reduces the magnetic field density. For a monopolar transmission line, the magnetic field density is higher (CIGRE, 2014).
- The currents at the poles they only contribute with its real component (CIGRE, 2014).

Using the previous considerations, the contributions of the magnetic field density due to the effect of the current in each of the components (horizontal and vertical) are obtained.

Figure 5 shows the horizontal and vertical components of the magnetic field at a point P, on the axis of the coordinates (x, y) located at a height of 1 m above the transmission line corridor (CIGRE, 2014), (IEEE, 2002).

The horizontal and vertical components are obtained by applying equations (3) and (4) respectively (CIGRE, 2014).

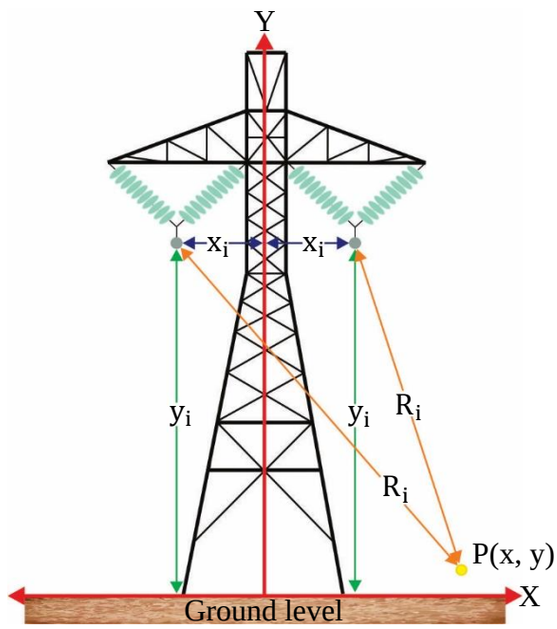

Figure 5 Horizontal and vertical components.
Source: Own elaboration

For the horizontal components, equation (3) is used.

$$B_{x_i} = \frac{\mu_0 \cdot I}{2 \times 10^{-6} \cdot \pi} \cdot \left(\frac{x - x_i}{R_i^2}\right) \mu T \quad (3)$$

For the vertical components, equation (4) is used.

$$B_{y_i} = \frac{\mu_0 \cdot I}{2\times10^{-6}\cdot\pi} \cdot \left(\frac{y-y_i}{R_i^{\,2}}\right) \mu T \quad (4)$$

Where:

B_{x_i} = Horizontal component of the pole magnetic field, in μT.
B_{y_i} = Vertical component of pole magnetic field, in μT.
μ_0 = Magnetic permeability of vacuum $4 \cdot \pi x10^{-7}$, in $\frac{H}{m}$.
X = Coordinate on the horizontal axis of the measurement point P, in m.
Y = Coordinate on the vertical axis of the measurement point P, in m.
x_i = Coordinate on the horizontal axis of the pole, in m.
y_i = Coordinate on the vertical axis of the pole, in m.
R_i = Distance between pole and measuring point P, in m.

The distance between the pole and the measurement point P, is obtained with equation (5).

$$R_i = \sqrt{(x-x_i)^2 + (y-y_i)^2}\ m \quad (5)$$

Sum of all contributions at a point

The magnetic field at the measurement point P, under the transmission line, will be the sum of the contributions from the poles and are obtained by applying equations (6) and (7) (CIGRE, 2014).

$$B_H = \sum_{i=1}^{u} B_{x_i}\ \mu T \quad (6)$$

$$B_V = \sum_{i=1}^{u} B_{y_i}\ \mu T \quad (7)$$

Where:

B_H = Horizontal component of magnetic field under the line at measurement point P, in μT.
B_V = Vertical component of magnetic field under the line at the measurement point P, in μT.
u = Number of poles present in the line.

The total magnetic field at the measurement point P is obtained by applying equation (8).

$$B_T = \sqrt{B_H^{\,2} + B_V^{\,2}}\ \mu T \quad (8)$$

Where:

B_T = Total magnitude of magnetic field at measurement P, in μT.

The International Commission on Non-Ionizing Radiation Protection (ICNIR) and the International Radiological Protection Association (IRPA) recommend that the limit of public exposure to magnetic field in transmission lines in HVDC should be less than 40 mT (ICNIRP, 2009).

Case study

Consider a 500 kV bipolar transmission line in HVDC where you want to calculate the density of the magnetic field at one meter above ground level, over a 120 m corridor of line. Table 1 shows the spatial measurements of the pole locations of the bipolar line. Figure 6 shows the configuration of the transmission tower, the spacing between the posts and its location above ground level. Table 2 shows the operating characteristics of the line.

Conductor	x axis	y axis
Positive pole	-10 m	20 m
Negative pole	10 m	20 m

Table 1 Coordinates of the poles in the bipolar transmission line
Source: Own elaboration

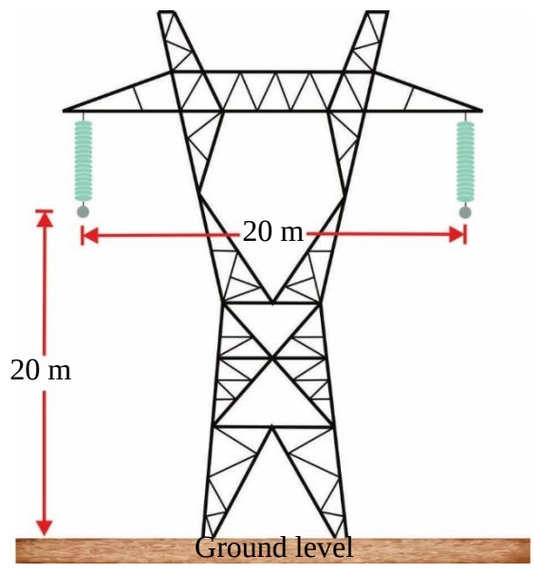

Figure 6 Profile of the 500 kV bipolar transmission line in HVDC
Source: (Lee, Pong & Zhu, 2019)

Operation characteristics	Value per unit
Tension electrical rating	500 kV
Electrical rated power	3000 MW
Type of conductor	ACSR 1590
Separation between poles	20 m
Height of the poles	20 m

Table 2 Specifications of the bipolar transmission line
Source: Own elaboration

Calculation of the electric current

The electric current is obtained using equation (1).

$$I = \frac{1}{2} \cdot \left(\frac{3000 \times 10^3}{500} \right) = 3000 \text{ A}$$

Calculation of horizontal and vertical components

The distance from the pole to the measurement point P is obtained by equation (5), IEEE recommends that the magnetic fields density calculation be considered at a height of 1 m above ground level along the transmission line corridor (IEEE, 1994), using intervals of 10 m from the line corridor.

Considering a point P (x = 0, y = 1), for the positive pole.

$$R_1 = \sqrt{(0 - (-10))^2 + (1 - 20)^2}$$
$$R_1 = 21.4709 \text{ m}$$

For the rest of the intervals of the line runner of the positive pole, the results shown in Table 3 are obtained.

Coordinates	Distance in, m
P (x= 0, y= 1)	$R_1 = 21.4709$
P (x= 10, y= 1)	$R_1 = 27.5862$
P (x= 20, y= 1)	$R_1 = 35.5105$
P (x= 30, y= 1)	$R_1 = 44.2831$
P (x= 40, y= 1)	$R_1 = 53.4883$
P (x= 50, y= 1)	$R_1 = 62.9364$
P (x= 60, y= 1)	$R_1 = 72.5327$

Table 3 Distance from the positive pole to the measurement point.

Performing the same procedure for the negative pole.

$$R_2 = \sqrt{(0 - 10)^2 + (1 - 20)^2}$$
$$R_2 = 21.4709 \text{ m}$$

For the rest of the intervals of the line runner of the negative pole, the results shown in Table 4 are obtained.

Coordinates	Distance in, m
P (x= 0, y= 1)	$R_2 = 21.4709$
P (x= 10, y= 1)	$R_2 = 19$
P (x= 20, y= 1)	$R_2 = 21.4709$
P (x= 30, y= 1)	$R_2 = 27.5862$
P (x= 40, y= 1)	$R_2 = 35.5105$
P (x= 50, y= 1)	$R_2 = 44.2831$
P (x= 60, y= 1)	$R_2 = 53.4883$

Table 4 Distance from pole 2 to the measurement point.

The calculation of the magnetic field components of each pole is carried out. For the positive pole, the distance R_1 to point P (x= 0, y= 1) is used, applying equations (3) and (4) as shown below.

$$B_{x_1} = \frac{\pi \cdot 4 \times 10^{-7} \cdot 3000}{2 \times 10^{-6} \cdot \pi} \cdot \left(\frac{0 - (-10)}{(21.4709)^2} \right)$$
$$B_{x_1} = 13.0151 \ \mu\text{T}$$

$$B_{y_1} = \frac{\pi \cdot 4 \times 10^{-7} \cdot 3000}{2 \times 10^{-6} \cdot \pi} \cdot \left(\frac{1 - 20}{(21.4709)^2} \right)$$
$$B_{y_1} = -24.7288 \ \mu\text{T}$$

The results obtained from the horizontal and vertical components of the positive pole are show in Table 5 and 6 respectively.

Coordinates	Component in, μT
P (x= 0, y= 1)	$B_{x_1} = 13.0151$
P (x= 10, y= 1)	$B_{x_1} = 15.7687$
P (x= 20, y= 1)	$B_{x_1} = 14.2743$
P (x= 30, y= 1)	$B_{x_1} = 12.2386$
P (x= 40, y= 1)	$B_{x_1} = 10.4858$
P (x= 50, y= 1)	$B_{x_1} = 9.0886$
P (x= 60, y= 1)	$B_{x_1} = 7.9832$

Table 5 Horizontal components of the positive pole on the line corridor

Coordinates	Component in, μT
P (x= 0, y= 1)	$B_{y_1} = -24.7288$
P (x= 10, y= 1)	$B_{y_1} = -14.9802$
P (x= 20, y= 1)	$B_{y_1} = -9.0404$
P (x= 30, y= 1)	$B_{y_1} = -5.8133$
P (x= 40, y= 1)	$B_{y_1} = -3.9846$
P (x= 50, y= 1)	$B_{y_1} = -2.8780$
P (x= 60, y= 1)	$B_{y_1} = -2.1668$

Table 6 Vertical components of the positive pole on the line corridor

ISSN: 2414-4924

For the negative pole, the distance R_2 to point P (x= 0, y= 1) is used, applying equations (3) and (4) as shown below.

$$B_{x_2} = \frac{\pi \cdot 4 \times 10^{-7} \cdot -3000}{2 \times 10^{-6} \cdot \pi} \cdot \left(\frac{0 - 10}{(21.4709)^2}\right)$$
$$B_{x_2} = 13.0151\ \mu T$$

$$B_{y_2} = \frac{\pi \cdot 4 \times 10^{-7} \cdot -3000}{2 \times 10^{-6} \cdot \pi} \cdot \left(\frac{1 - 20}{(21.4709)^2}\right)$$
$$B_{y_2} = 24.7288\ \mu T$$

The results obtained from the horizontal and vertical components of the negative pole are show in Table 7 and 8 respectively.

Coordinates	Component in, μT
P (x= 0, y= 1)	$B_{x_2} = 13.0151$
P (x= 10, y= 1)	$B_{x_2} = 0$
P (x= 20, y= 1)	$B_{x_2} = -13.0151$
P (x= 30, y= 1)	$B_{x_2} = -15.7687$
P (x= 40, y= 1)	$B_{x_2} = -14.2743$
P (x= 50, y= 1)	$B_{x_2} = -12.2386$
P (x= 60, y= 1)	$B_{x_2} = -10.4858$

Table 7 Horizontal components of the negative pole on the line corridor

Coordinates	Component in, μT
P (x= 0, y= 1)	$B_{y_2} = 24.7288$
P (x= 10, y= 1)	$B_{y_2} = 31.5789$
P (x= 20, y= 1)	$B_{y_2} = 24.7288$
P (x= 30, y= 1)	$B_{y_2} = 14.9802$
P (x= 40, y= 1)	$B_{y_2} = 9.0404$
P (x= 50, y= 1)	$B_{y_2} = 5.8133$
P (x= 60, y= 1)	$B_{y_2} = 3.9846$

Table 8 Vertical components of the negative pole on the line corridor

Sum of all contributions at a point

The sum of the contributions for the horizontal component at the measurement point P (x= 0, y= 1), is developed using equation (6).

$$B_H = 13.0151 + 13.0151 = 26.0302\ \mu T$$

Table 9 shows the results obtained from the contributions for the horizontal component on the line corridor.

Coordinates	Component in, μT
P (x= 0, y= 1)	$B_H = 26.0302$
P (x= 10, y= 1)	$B_H = 15.7687$
P (x= 20, y= 1)	$B_H = 1.2592$
P (x= 30, y= 1)	$B_H = -3.5300$
P (x= 40, y= 1)	$B_H = -3.7885$
P (x= 50, y= 1)	$B_H = -3.1500$
P (x= 60, y= 1)	$B_H = -2.5025$

Table 9 Contributions of the horizontal component

The sum of the contributions for the vertical component at the measurement point P (x = 0, y = 1), is developed using equation (7).

$$B_V = -24.7288 + 24.7288 = 0\ \mu T$$

Table 10 shows the results obtained from the contributions for the vertical component on the line corridor.

Coordinates	Component in, μT
P (x= 0, y= 1)	$B_V = 0$
P (x= 10, y= 1)	$B_V = 16.5986$
P (x= 20, y= 1)	$B_V = 15.6884$
P (x= 30, y= 1)	$B_V = 9.1669$
P (x= 40, y= 1)	$B_V = 5.0558$
P (x= 50, y= 1)	$B_V = 2.9352$
P (x= 60, y= 1)	$B_V = 1.8177$

Table 10 Vertical component contributions

Finally, the total magnitude of the magnetic field is calculated at the measurement point P (x = 0, y = 1), using equation (8).

$$B_T = \sqrt{(26.0302)^2 + (0)^2} = 26.0302\ \mu T$$

Table 11 shows the results obtained from the total magnitude of the magnetic field on the line corridor.

Coordinates	Magnetic field density in, μT
P (x= 0, y= 1)	$B_T = 26.0302$
P (x= 10, y= 1)	$B_T = 22.8947$
P (x= 20, y= 1)	$B_T = 15.7388$
P (x= 30, y= 1)	$B_T = 9.8231$
P (x= 40, y= 1)	$B_T = 6.3177$
P (x= 50, y= 1)	$B_T = 4.3056$
P (x= 60, y= 1)	$B_T = 3.0930$

Table 11 Magnetic field density over the line corridor

In Figure 7, the plotted results of the magnetic field density over the corridor of the 500 kV bipolar transmission line in HVDC are presented.

ISSN: 2414-4924

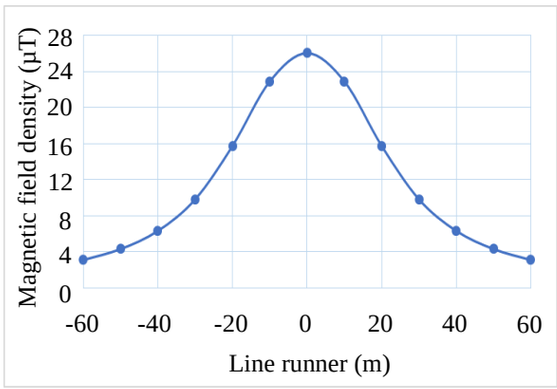

Figure 7 Magnetic field density of the 500 kV bipolar transmission line in HVDC

In Figure 7 it is observed that for the transmission line under study, the maximum magnetic field intensity is 26.0302 μT, which is lower than the maximum limit recommended by the ICNIRP.

Results

To obtain a validation of the methodology presented to calculate the density of the magnetic field, a simulation of the transmission line under study is carried out, for this the FACE software (FACE, 2019) was used, since it allows the configuration of the profiles. Transmission lines. This software is based on the complex penetration method, which uses the Carson method, which consists of the circulation of a current that returns through the earth, this method considers the earth as a superconductor, with which the return of current through the earth is modeled. Unlike the methodology presented, the FACE software uses the image conductor effect.

Table 12 and Figure 8 show the comparison of the results obtained between the methodology presented and the validation of the FACE software.

Magnetic field density	
Methodology in, μT	**FACE in, μT**
$B_{T0} = 26.0302$	$B_{T0} = 25.7698$
$B_{T10} = 22.8947$	$B_{T10} = 22.6657$
$B_{T20} = 15.7388$	$B_{T20} = 15.5814$
$B_{T30} = 9.8231$	$B_{T30} = 9.7248$
$B_{T40} = 6.3177$	$B_{T40} = 6.2545$
$B_{T50} = 4.3056$	$B_{T50} = 4.2625$
$B_{T60} = 3.0930$	$B_{T60} = 3.0620$

Table 12 Comparison of the results obtained between the methodology and the FACE software

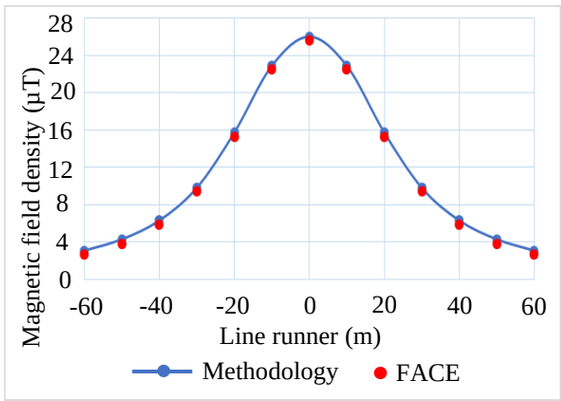

Figure 8 Comparison of the results obtained between the methodology and the FACE software

The percentage difference between the results obtained by the methodology and the FACE software is obtained with equation (9).

$$\text{dif}\,\% = \frac{M-F}{F} \cdot 100\ \% \qquad (9)$$

Where:

M = Magnetic field density obtained by the methodology proposed here, in μT.

F = Magnetic field density obtained by FACE software, in μT.

The comparison of the results obtained in interval 0 on the line corridor presented in Figure 8 and in Table 12 is made, using equation (9).

$$\text{dif}\,\% = \frac{26.0302 - 25.7698}{25.7698} \cdot 100$$

$$\text{dif}\,\% = 1.0104\%$$

Table 13 shows the percentage difference between the results obtained by the methodology and the FACE software, on the intervals of the line corridor.

Line runner intervals in, m	Percentage difference in, %
0	1.0104
10	1.0103
20	1.0101
30	1.0108
40	1.0104
50	1.0111
60	1.0124

Table 13 Percentage difference of the results obtained between the methodology and the FACE software

Analysis of the impact of the line configuration on the magnetic field density

For the analysis of the transmission line, two additional spatial configurations to the one presented in Table 1 are considered, to determine the most efficient configuration and obtain a smaller tower with a shorter line corridor.

Table 14 shows the coordinates of the poles of the second configuration of the line.

Conductor	x axis	y axis
Positive pole	-8 m	15 m
Negative pole	8 m	15 m

Table 14 Coordinates of the poles of the second configuration of the bipolar transmission line

Carrying out the methodology procedure with the second configuration of the line presented in Table 14, the results of the magnetic field density shown in Figure 9 are obtained.

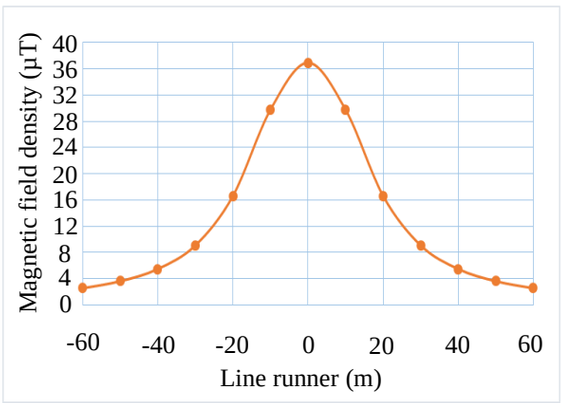

Figure 9 Magnetic field density of the second configuration of the 500 kV bipolar transmission line in HVDC

The behavior of the results obtained are typical of a transmission line, as presented in (Ahmed, Wael & Ehab, 2012).

Table 15 shows the coordinates of the poles of the third configuration of the line.

Conductor	x axis	y axis
Positive pole	-12.5 m	25 m
Negative pole	12.5 m	25 m

Table 15 Coordinates of the poles of the third configuration of the bipolar transmission line

Performing the methodological procedure with the third configuration shown in Table 15, the results of the magnetic field density shown in Figure 10 are obtained.

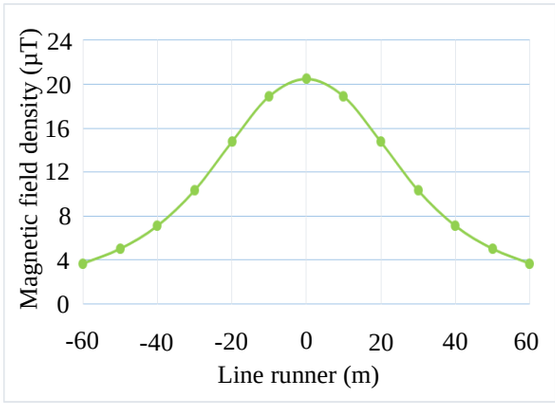

Figure 10 Magnetic field density of the third configuration of the 500 kV bipolar transmission line in HVDC

Figure 11 shows the change in the density of the magnetic field of the presented configurations, as a function of the dimensions of the tower (spacing and height) and the position of the points P.

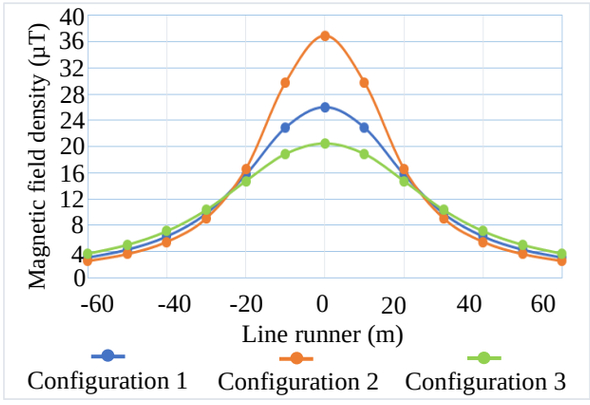

Figure 11 Magnetic field density of configurations 1, 2 and 3

The results of the magnetic field density for configurations 1, 2 and 3 are shown in Figures 7, 9 and 10, respectively, in Figure 11 the comparison of the results is observed. Configuration 3 has a lower magnetic field density, but because the transmission line has an increase in height and a greater separation of its poles, an economic increase in its installation will be generated. Due to this, it is verified that the most efficient configuration is the one presented in configuration 1 of the case study.

ISSN: 2414-4924

Conclusions

The following points are concluded from the work carried out:

- A reference methodology is presented, containing the steps necessary to perform the calculation of the magnetic field density, for the first HVDC overhead transmission lines to be built in Mexico.

- The methodology presented may be applied in bipolar and monopolar lines, admitting the different nominal voltages of the lines in HVDC, allowing to calculate the magnetic field density at a height between the poles and the ground level, over the transmission line corridor.

- The use of the presented methodology offers speed and precision, unlike commercial software like FACE generates a calculation memory of the magnetic field density in the corridor of the transmission line under study for free.

- The magnetic field density profile was validated of the 500 kV bipolar transmission line in HVDC with the FACE software, with which a difference of 1% is obtained, Because the software uses the effect of image conductor and the presented methodology does not consider it, since the effect is so small that it can be overlooked.

- It is determined that the geometry of the transmission line under study will not present magnetic field problems, as the results are less than the maximum limit recommended by the ICNIRP.

- Magnetic field density increases as the height of the poles decreases and will decrease as the distance between the poles increases.

References

Ahmed, H. Wael, M. & Ehab, M. (2012). Effect of Electromagnetic fields from Power Lines on Metallic Objects and Human Bodies.

Baharman, M. & Johnson, B. (2007). The ABCs of HVDC transmission technologies. IEEE Power and Energy Magazine.

CIGRE. (2014). CIGRE green book & overhead lines. Paris, France.

FACE. (2019). Field and corona effects, Manitoba hydro international. Canada.

Feltes, J. Gemmell, B. & Retzmann, D. (2011). From smart grid to super grid: Solutions with HVDC and FACTS for grid access of renewable energy sources. IEEE Power and Energy Society General Meeting.

Girdinio, P. Molfino, P. Nervi, M. Rossi, M. Bertani, A. & Malgarotti, S. (2015). Technical and Compatibility issues in the Design of HVDC Sea Electrodes. International Symposium on Electromagnetic Compatibility.

ICNIRP. (2009). Guidelines on limits of exposure to static magnetic fields.

IEC. (2014). IEC 62681 Electromagnetic performance of high voltage direct current (HVDC) overhead transmission lines.

IEEE. (2002). IEEE STD C95.6 Safety levels with respect to human exposure to electromagnetic fields, 0-3 kHz.

IEEE. (1994). IEEE STD Procedures for measurement of power frequency electric and magnetic fields from power lines.

Jang, Gil. Kim, Chan. Lee, Seok. Lim, Seong. & Sood, Vijay. (2009). HVDC transmission power conversion applications in power systems. John wiley & sons (Asia).

Lee, W. Pong, Philip. & Zhu, Ke. (2019). Non-contact voltage monitoring of HVDC transmission lines based on electromagnetic fields. IEEE Sensors journal, Vol. 19, No. (8).

Mooney, J. (2010). Electrical considerations for HVDC transmission lines. Power Engineers, Registered Continuing Education program RCEP.

ISSN: 2414-4924

PRODESEN. (2019). Programa de ampliación y modernización de la red nacional de transmisión y redes generales de distribución del mercado eléctrico mayorista 2019-2033.

Rofalski, K. & Schlabbach, J. (2014). Power system engineering, planning, design, and operation of power systems and equipment. John wiley & sons.

Samy, M. (2017). Computation of electromagnetic fields around HVDC transmission line tying Egypt and ksa. IEEE Nineteenth international middle aast power systems conference. Egypt.

Sarma, Maruvada, P. (2000). Corona performance of high-voltage transmission lines. Canada.

Tang, G. Luo, X. & Wei, X. (2013). Multi-terminal HVDC and DC-grid technology. Proc. Chi. Socie. Elect. Eng.

Zhou, H. Qiu, W. Sun, K. Chen, J. Deng, X. Qian, F. Wang, D. Zhao, B. Li, J. Li, S. Qiu, Y. & Yu, J. (2018). Ultra-high voltage AC/DC power transmission.

Zhu, K. Lee, W. K. & Pong, P. W. T. (2018). Fault-Line Identification of HVDC Transmission Lines by Frequency-Spectrum Correlation Based on Capacitive Coupling and Magnetic Field Sensing. IEEE Trans. Magn.

ISSN: 2414-4924